

Simulation of Rare Events in Images

Shruthi S. Kubatur¹ and Mary L. Comer²

¹Nikon Research Corporation of America, Belmont, CA, and ²Purdue University, West Lafayette, IN

Abstract

Many important physical processes in fields such as materials science, ecology, structural biology, and clinical pathology involve the study of microscopic structures – from formation and propagation to steady-state behavior. The study of these phenomena is often very slow, creating an enormous need for accurate computer simulation of the underlying processes.

In this paper, we provide a robust algorithm for simulation of images of such processes modeled by a Gibbs distribution. As part of our rare-event simulation solution, we adapt an importance sampling technique specifically for Markov random fields. We conclude by showing results of simulation of images of abnormal grain growth in poly-crystalline materials and NiCrAl super-alloy precipitates that find applications in several important real-life fields such as aircraft material design.

Introduction

MANY important physical processes studied by scientists in a variety of fields such as materials science, structural biology, and clinical pathology involve the study of microscopic structures – from formation and propagation to steady-state behavior [1, 2, 3]. Unfortunately, direct observation of such phenomena are very slow and impractical, thus necessitating accurate simulation of the images that capture these phenomena. Even though the processes are stochastic in nature, there is still an underlying model that is at play. A simple but effective way to analyze these processes is through the energy of the system. Almost all natural systems that evolve over time do so in a way that reduces the net system energy (also known as the *hamiltonian*).

In any case, useful stochastic simulation depends on accurate stochastic modeling using appropriate probability distributions. For images that contain normal/expected structures, effective simulation methods have been developed previously. In fact, there exists an entire class of Markov chain Monte Carlo (MCMC) methods [4, 5, 6, 7] that allow us to sample images that contain structures modeled by a variety of probability distributions. However, these methods are not effective when images deviate significantly from expected behavior.

In many applications, it is important to study certain abnormal events that occur very rarely [8, 9, 10]. However, modeling rare events using traditional statistics is usually not feasible. For typical behavior, empirical distributions (often in the form of histograms) can be computed from experimental data. Probability distributions can be fit to histograms, and statistical tests can measure goodness-of-fit. For a rare event, on the other hand, the number of experiments needed to compute reasonable probability estimates can be astronomically large. This problem becomes especially difficult for modeling rare events in a high-dimensional space, such as images. Such cases often requiring some form of

the Gibbs distribution,

$$p(x) = \frac{1}{Z} \exp(-U(x)), \quad (1)$$

where x represents the higher-dimension configuration, Z is the partition function, and $U(x)$ is the system energy of x .

In this paper, we build upon our simulation methods [11, 12] to formulate a generic rare-event image simulation framework based on importance sampling. We wish to emphasize that the theory developed throughout this paper is general and can be applied to a wide variety of modeling and simulation problems, though we choose to show two important imaging applications pertaining to important materials science phenomena. Specifically, we describe how to simulate images of abnormal grain growth in polycrystalline materials and images of overlapping super-ellipses that model NiCrAl super-alloy precipitates – both of whose underlying processes can be modeled by Gibbs distribution.

Our first application is the growth of grains in a polycrystalline material, which is a very complex phenomenon. In recent years, many computational methods have been developed to simulate grain evolution, and to study the effects of grain growth on the overall properties of a material. One such method uses the Ising/Potts model, with simulation based on Metropolis sampling [13, 14]. For our second application, we are interested in applying our rare-event simulation algorithm to simulate images of overlapping precipitates in nickel-based super-alloys. As an example, we work with the nickel-chromium-aluminum (NiCrAl) super-alloy [15, 16]. To model the shape of these precipitates, we adopt super-ellipses inspired by [15].

In the Background section, we briefly outline spatial point processes, marked point processes, and importance sampling to give the reader some necessary background to appreciate the paper better. In the Method section, we begin by expressing our materials science problems as random experiments using Gibbs distributions and marked point processes (MPP) [17, 18]. It turns out that abnormally large grains and overlapping NiCrAl precipitates occur with a low probability, and as such the Gibbs distribution that models normal behavior cannot be directly used within the Metropolis-Hastings algorithm. To address this issue, we adapt an importance sampling strategy for our Gibbs distribution. This involves modifying the way we compute the system energy of the 2D configurations in our images.

Finally, in the Results section, we present several image simulation results showing configurations corresponding to various parameter combinations. Finally, we demonstrate the effectiveness of our maximum likelihood parameter estimation followed by results from the anomaly detection experiment.

Background

Spatial Point Processes and MPP

Spatial point processes are random processes that model how points are distributed in a 1D, 2D or 3D space. Point processes describe certain characteristics such as the number of points, and interaction between these points in a random pattern. Marked point processes (MPP) are an extension of spatial point processes, which assign marks to the points to describe properties. MPPs have several applications such as object detection [19, 20], image analysis and reconstruction [21, 22], and denoising [23].

Importance Sampling

Suppose X is a random variable describing a random experiment on a sample space, with probability density given by $p(x)$. We are interested in evaluating the probability:

$$\rho = \mathbb{E}[\mathbb{1}_A(X)], \quad (2)$$

where $\mathbb{1}_A(x)$ is an indicator function on the set A which is of interest to us. One way to evaluate Eq. 2 is to sample n i.i.d. random variables X_1, X_2, \dots, X_n from $p(x)$ and calculate,

$$\hat{\rho} = \frac{1}{n} \sum_{i=1}^{i=n} \mathbb{1}_A(X_i). \quad (3)$$

Here, $\hat{\rho}$ is known as the Monte Carlo estimate. An alternative way to evaluate Eq. 2 is to sample n i.i.d. random variables X_1, X_2, \dots, X_n from a distribution $q(x)$ known as the importance sampling distribution, and to calculate the estimate,

$$\hat{\rho}_{IS} = \frac{1}{n} \sum_{i=1}^{i=n} \mathbb{1}_A(X_i) \frac{p(X_i)}{q(X_i)}. \quad (4)$$

Here, $\hat{\rho}_{IS}$ is known as the importance sampling estimate, and $q(x)$ is such that $\mathbb{1}_A(x)q(x)$ is non-zero for values of x at which $\mathbb{1}_A(x)p(x)$ is non-zero. The ratio $\frac{p(\cdot)}{q(\cdot)}$ in Eq. 4 is called the Radon-Nikodym correction term. This term is introduced to correct for the artificially boosted probability obtained because of choosing an importance sampling distribution $q(\cdot)$ instead of the original distribution $p(\cdot)$. We must choose the importance sampling density carefully. Ideally, the importance sampling density should be such that it hits the rare event of interest A more often. It can be seen that $\mathbb{E}_q[\hat{\rho}_{IS}] = \rho$ implying $\hat{\rho}_{IS}$ is an unbiased estimator of ρ .

Method

Importance Sampling to Simulate Abnormal Grain Growth Images

In this section, we formulate an expression for the importance sampling-specific interaction potential, $G(s)$, and hence the full system potential, $W(s)$. For our purpose, $G(s)$ must satisfy two conditions - it must be a measure of abnormality of the configuration, and it must have a form that can be summed over all the lattice sites in the configuration.

But what does it mean for $G(s)$ to measure the amount of abnormality in configuration s ? A zeroth order approach would be for $G(s)$ to be a count of all sites in the configuration s that belong to the (most) abnormal grain¹ (with grain index k_{abn}). A better

¹This would raise the question of what would make a grain (the most) abnormal. We answer this important question after we develop an expression for $G(s)$, and we assume for now that we have a grain, $g_{k_{abn}}$, that is abnormally growing.

expression of $G(s)$ would not only count sites that belong to the abnormal grain, but also weight each count by *the abnormality of the neighborhood of each site*. The abnormality of the neighborhood could simply be a count of the number of neighboring lattice sites that belong to the abnormal grain. The second condition on $G(s)$ ensures that updating $G(s)$ (after every lattice site update in the Metropolis-Hastings algorithm) would be computationally tractable.

With these considerations in mind, our proposed expression for $G(s)$ is as follows,

$$G(s) = \sum_{i=1}^N c_i(n_i + 1), \quad (5)$$

where, N is the number of sites in the lattice,

$$c_i = \begin{cases} c_1 & \text{if site } i \text{ belongs to the } k_{abn}\text{-th grain} \\ c_2 & \text{otherwise} \end{cases}$$

c_1, c_2 are constants such that $c_1 > c_2$.

n_i = number of neighboring sites of i that belong to the k_{abn} -th grain.

k_{abn} is the index of the most abnormally growing grain.

Note that the term $(n_i + 1)$ in Eq. (5) guards against the case when none of the neighbors of site i belong to the abnormal grain, as opposed to having just n_i which would zero out $G(s)$ even when site i belongs to the abnormal grain.

We calculate the index, k_{abn} , of the (most) abnormal grain by considering two factors:

- (1) the size of the grains in configuration s , and
- (2) the velocity at which the grains are growing.

Specifically, we compute the abnormal grain index by a very simple two-objective optimization as follows:

$$k_{abn} = \arg \max_k (s_k + wv_k^{(p)}), \quad (6)$$

where s_k is the size of the k -th grain, $v_k^{(p)}$ is its velocity, and the weight, w , balances the size and velocity. In order to make an assessment of how fast the grains are growing *currently*, we use the notion of “instantaneous” velocity. The (instantaneous) velocity, $v_k^{(p)}$, of grain k can be defined as the net growth of the grain k in the past p attempts².

To simulate abnormal grain growth, we use a modified system potential given by $W(s) = E(s) - gG(s)$, where g is a user-chosen parameter and $E(\cdot)$ denotes the Markov random field system energy [12].

Putting all results together, the importance sampling density π_W can be explicitly written as,

$$\pi_W(s) = \frac{1}{Z} \exp\left(\frac{-(E(s) - g^*G(s))}{k_B T}\right), \quad (7)$$

where $E(s) = \sum_{i=1}^N \sum_{j=1}^z \gamma_{ij}$ and $G(s) = \sum_{i=1}^N c_i(n_i + 1)$, and g^* is the optimal value of parameter g .

²The value of $p = 1$ would be make the velocity highly instantaneous, but is not usually the best choice because of possible fluctuations. On the other hand, a high value of p makes the velocity less instantaneous and possibly “misleading”.

Importance Sampling to Simulate Overlapping NiCrAl Super-Ellipse Images

Our objective is to simulate a marked point process X with probability distribution $p(\cdot)$. We define $P \subset \mathbb{Z}^2$ to be a $P_1 \times P_2$ discrete lattice which is the space of points upon which we wish to simulate our marked point process. Let $M \subset \mathbb{R}^3$ be the space of marks associated with the points. Then, $\mathcal{X} = P \times M$ is the space of all marked points, upon which we wish to simulate a set of objects. Suppose, x is the realization of X then $x \in \{x_n = (p_n, m_n) : p_n \in P, m_n \in M\}$.

Let N_x denote the number of objects and S_x denote the amount of clustering in a realization x of the marked point process X . N_x and S_x are random variables since they are realized through a random process.

Based on [24], the marked point process can be described through a Gibbs density function,

$$f(x) = \frac{1}{Z} \exp\left(-\frac{1}{kT}U(x)\right), \quad (8)$$

where $U(x)$ is known as the Gibbs potential and Z is the normalizing constant called the partition function, k is the Boltzmann constant, and T is the temperature.

One possible MPP model is the Strauss model which is based on the number of objects and pairwise interaction of objects in the random process. The Gibbs potential for the Strauss model [24] is given by,

$$U(x) = \lambda N_x + \beta \left(\sum_{\{i,j\}} 1_{[0,d]} \left(\|p_i - p_j\|_2^2 \right) \right), \quad (9)$$

where $\lambda \geq 0$ controls the number of super-ellipses in our simulation, $\beta \geq 0$ controls how clustered or dispersed the spatial points are, $d > 0$ is the clustering radius of the spatial points.

This Strauss model does a good job of characterizing the underlying spatial point pattern. Since our objective is to simulate configurations with specific amounts of overlap between objects of different sizes, we add another term to the Gibbs potential to control the amount of overlap. The resulting Gibbs potential is,

$$U(x) = \lambda N_x + \beta \left(\sum_{\{i,j\}} 1_{[0,d]} \left(\|p_i - p_j\|_2^2 \right) \right) + \gamma_1 \sum_{i,j} R(w_i, w_j), \quad (10)$$

where $R(w_i, w_j)$ is the normalized overlap area between objects w_i and w_j in configuration x and γ_1 is the parameter that controls the overlap between objects.

Let $S_x = \sum_{\{i,j\}} 1_{[0,d]} \left(\|p_i - p_j\|_2^2 \right)$ and $R_x = \sum_{i,j} R(w_i, w_j)$. Then the Gibbs potential can be rewritten as,

$$U(x) = \lambda N_x + \beta S_x + \gamma_1 R_x. \quad (11)$$

Therefore, the Gibbs density function for our model is given by,

$$f(x) = \frac{1}{Z} \exp\left(-(\lambda N_x + \beta S_x + \gamma_1 R_x)\right). \quad (12)$$

For both abnormal grain growth and overlapping super-ellipses, once we have a target importance sampling density function, we use the Metropolis-Hastings algorithm [25] to draw samples (i.e., images in our case) from it.

Results and Discussion Abnormal Grain Growth Simulation

We perform nine simulations by varying the value of the importance sampling parameter, g^* . In order to observe the effect g^* has on the microstructure evolution, we keep other parameters (velocity weight w , c^1 , and c^2) fixed. Specifically, we set $c^1 = 1$, $c^2 = -1$, and $w = 0.8$. We then vary g^* from 0 to 0.24 in steps of 0.03. The case where $g^* = 0$ corresponds to having no importance sampling potential term ($G(s)$), and our simulation falls back to the regular Monte Carlo framework. For each simulation s , we report the fraction of the area occupied by the largest grain.

In our experimental results, we observe that the largest grain size increases with increasing values of g^* . This property helps us solve for the required value of g^* empirically, given the knowledge of desired value of the largest grain size. Since we experiment with a limited number of g^* values, we perform a curve fitting operation to establish the relationship between g^* and the largest grain size.

We fit a degree-3 polynomial that fits the data best (in the least squares sense), and the resultant curves are given in Fig. 2. Suppose, we are interested in generating a configuration with an abnormal grain that occupies about 30% of the total area (i.e., $t = 0.3$), then the required value of the IS parameter g would be approximately 0.16. This is as shown in Fig. 2.

The curve fitted to a polynomial of degree 3 is given by,

$$p_3(g) = 17.4585g^3 + 8.1510g^2 - 0.2820g + 0.0689. \quad (13)$$

NiCrAl Super-Ellipse Simulation

In this section, we present several simulation results showing configurations corresponding to various parameter combinations. These results highlight the effect of varying each parameter, holding the other two fixed. Then we vary just γ to simulate abnormal (overlapping) super-ellipses. Finally, we demonstrate the effectiveness of our maximum likelihood parameter estimation followed by results from the anomaly detection experiment.

Note that γ is a variable contraction that is composed of γ_1 and γ_2 as $\gamma := \gamma_2 - \gamma_1$. Regardless of the experiment, γ_1 is set to 2000, while only γ_2 is varied. So, for example, when we report a γ value of -200, we mean that we set $\gamma_2 = 1800$, maintaining γ_1 at 2000.

In summary, we have a reliable set of algorithms for stochastic simulation of normal and abnormal configurations.

Conclusion

In this paper, we provided a robust algorithm for simulation of images of physical processes that occur in natural systems in materials science, clinical pathology, etc. We modeled two specific materials science examples using a Gibbs distribution.

To develop our rare-event simulation solution, we adapted the method of importance sampling specifically for Gibbs distributions. Specifically, we showed several results of simulation of images of abnormal grain growth in poly-crystalline materials followed by evolution of NiCrAl super-alloy precipitates that find applications in several important real-life fields such as aircraft material design. With this, we propose a generic and effective method to simulate rare images in any system that can be characterized by Gibbs distributions.

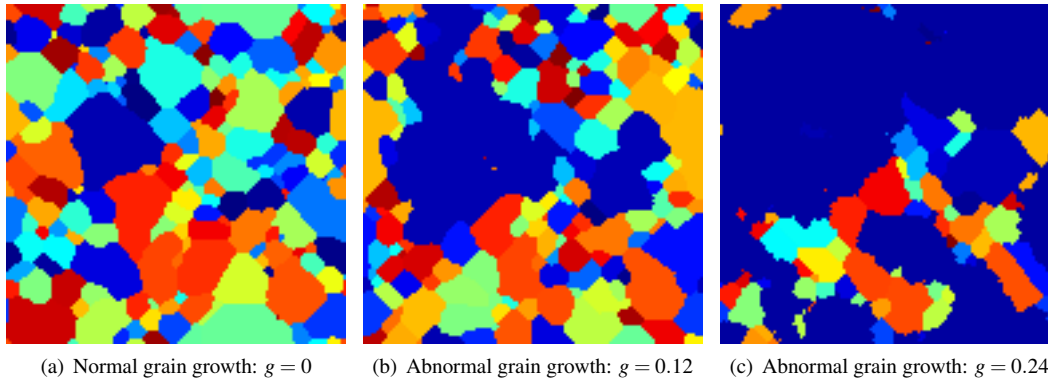


Figure 1: As we increase g , the area of the largest grain – visualized in blue – increases as well, from 5.2% in (a) to 19.8% in (b) to 66.7% in (c). All percentages are relative to the full lattice area.

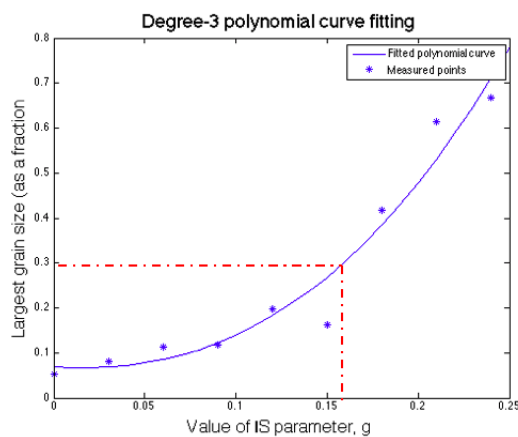


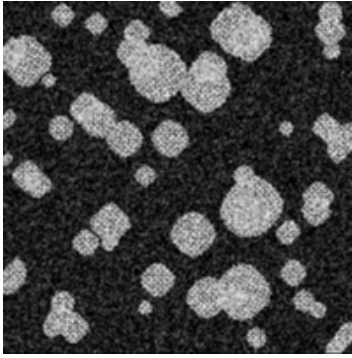
Figure 2: Degree-3 polynomial curve fitting to establish an empirical relationship between desired values of the largest grain size and corresponding required value of parameter g .

Acknowledgment

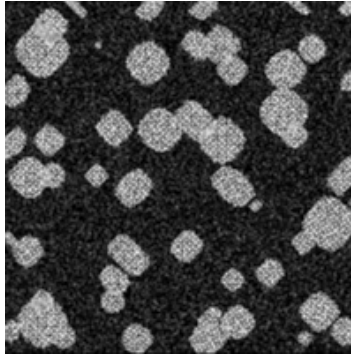
This research was undertaken when S. Kubatur was a PhD student at Purdue University and the authors were supported by the Air Force Office of Scientific Research contract #FA9550-14-1-0313. The authors also thank Prof. Marc De Graef of Carnegie Mellon University for NiCrAl images.

References

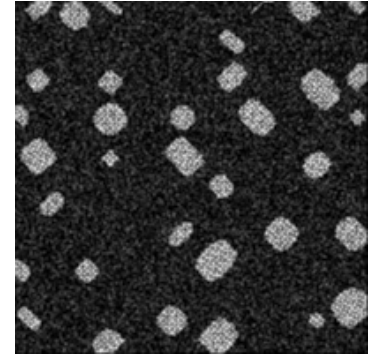
- [1] L.-Q. Chen, “Phase-field models for microstructure evolution,” *Annual review of materials research*, vol. 32, no. 1, pp. 113–140, 2002.
- [2] A. R. Roosen and W. C. Carter, “Simulations of microstructural evolution: anisotropic growth and coarsening,” *Physica A: Statistical Mechanics and its Applications*, vol. 261, no. 1, pp. 232–247, 1998.
- [3] T. A. Steitz, “Structural biology: A mechanism for all polymerases,” *Nature*, vol. 391, no. 6664, pp. 231–232, 1998.
- [4] W. K. Hastings, “Monte Carlo sampling methods using Markov chains and their applications,” *Biometrika*, vol. 57, no. 1, pp. 97–109, 1970.
- [5] D. Gamerman and H. F. Lopes, *Markov chain Monte Carlo: stochastic simulation for Bayesian inference*. CRC Press, 2006.
- [6] C. J. Geyer, “Practical Markov chain Monte Carlo,” *Statistical Science*, pp. 473–483, 1992.
- [7] P. Brémaud, *Markov chains: Gibbs fields, Monte Carlo simulation, and queues*. Springer Science & Business Media, 2013, vol. 31.
- [8] E. Weinan, W. Ren, and E. Vanden-Eijnden, “String method for the study of rare events,” *Physical Review B*, vol. 66, no. 5, p. 052301, 2002.
- [9] G. King and L. Zeng, “Explaining rare events in international relations,” *International Organization*, vol. 55, no. 03, pp. 693–715, 2001.
- [10] I.-J. Bae and S. Baik, “Abnormal grain growth of alumina,” *Journal of the American Ceramic Society*, vol. 80, no. 5, pp. 1149–1156, 1997.
- [11] S. S. Kubatur and M. L. Comer, “Rare event simulation for Markov random fields with application to grain growth in crystals,” in *Image Processing (ICIP), 2016 IEEE International Conference on*. IEEE, 2016, pp. 3748–3752.
- [12] —, “Simulation of abnormal grain growth in polycrystalline materials,” *Electronic Imaging*, vol. 2016, no. 19, pp. 1–9, 2016.
- [13] E. Holm and C. Battaile, “The computer simulation of microstructural evolution,” *JOM*, vol. 53, no. 9, pp. 20–23, 2001. [Online]. Available: <http://dx.doi.org/10.1007/s11837-001-0063-2>
- [14] M. A. Miodownik, “A review of microstructural computer models used to simulate grain growth and recrystallisation in aluminium alloys,” *Journal of Light Metals*, vol. 2, no. 3, pp. 125 – 135, 2002, modelling of Light Metals.
- [15] J. MacSleynne, M. Uchic, J. Simmons, and M. De Graef, “Three-dimensional analysis of secondary γ' precipitates in rené-88 dt and umf-20 superalloys,” *Acta Materialia*, vol. 57, no. 20, pp. 6251–6267, 2009.
- [16] G. Sabol and R. Stickler, “Microstructure of Nickel-based superalloys,” *physica status solidi (b)*, vol. 35, no. 1, pp. 11–52, 1969.
- [17] J. F. C. Kingman, *Poisson processes*. Wiley Online Library, 1993.
- [18] A. Penttinen, D. Stoyan, and H. M. Henttonen, “Marked point processes in forest statistics,” *Forest science*, vol. 38, no. 4, pp. 806–824, 1992.
- [19] W. Ge and R. T. Collins, “Marked point processes for crowd counting,” in *Computer Vision and Pattern Recognition*,



(a) $\lambda = -0.60, \beta = 0.40, \gamma = -5$; Super-ellipses: 57, Clustering: 123, Overlap: 37.37



(b) $\lambda = -0.60, \beta = 0.40, \gamma = -20$; Super-ellipses: 53, Clustering: 101, Overlap: 9.47



(c) $\lambda = -0.60, \beta = 0.40, \gamma = -200$; Super-ellipses: 36, Clustering: 51, Overlap: 0.58

Figure 3: Simulation of NiCrAl super-ellipses with three parameter combinations. (a), (b), and (c): normalized overlap monotonically decreases as we decrease γ keeping λ and β fixed.

2009. *CVPR 2009. IEEE Conference on*. IEEE, 2009, pp. 2913–2920.

- [20] F. Chatelain, A. Costard, and O. J. Michel, “A Bayesian marked point process for object detection. application to muse hyperspectral data,” in *2011 IEEE International Conference on Acoustics, Speech and Signal Processing (ICASSP)*. IEEE, 2011, pp. 3628–3631.
- [21] X. Descombes and J. Zerubia, “Marked point process in image analysis,” *IEEE Signal Processing Magazine*, vol. 19, no. 5, pp. 77–84, 2002.
- [22] N. Haala and M. Kada, “An update on automatic 3D building reconstruction,” *ISPRS Journal of Photogrammetry and Remote Sensing*, vol. 65, no. 6, pp. 570–580, 2010.
- [23] J.-L. Starck, E. J. Candès, and D. L. Donoho, “The curvelet transform for image denoising,” *IEEE Transactions on image processing*, vol. 11, no. 6, pp. 670–684, 2002.
- [24] A. Baddeley, J.-F. Coeurjolly, E. Rubak, and R. Waagepetersen, “Logistic regression for spatial Gibbs point processes,” *Biometrika*, p. ast060, 2014.
- [25] C. J. Geyer and J. Møller, “Simulation procedures and likelihood inference for spatial point processes,” *Scandinavian Journal of Statistics*, pp. 359–373, 1994.

Author Biography

Shruthi S. Kubatur received her PhD in electrical engineering from Purdue University – West Lafayette, IN (2017). Since then, she has been working as Sr. Computer Scientist Engineer at Nikon Research Corporation of America in Belmont, CA. Her research interests and work have ranged from pattern recognition and image segmentation to rare event simulation.

Mary L. Comer received her PhD in electrical engineering from Purdue University – West Lafayette, IN (1995). She is currently Associate Professor of Electrical and Computer Engineering at Purdue University, where she has worked on image modeling and segmentation, image analysis, video coding, probability theory, and rare-event simulation.